Difficulties in analytic computation for relative entropy of entanglement

Hungsoo Kim,[1] Mi-Ra Hwang,[2] Eylee Jung,[2] and DaeKil Park[2,3]
[1]*The Institute of Basic Science, Kyungnam University, Masan 631-701, Korea*
[2]*Department of Physics, Kyungnam University, Masan 631-701, Korea*
[3]*Department of Electronic Engineering, Kyungnam University, Masan 631-701, Korea*
(Received 25 February 2010; published 19 May 2010)

It is known that relative entropy of entanglement for an entangled state ρ is defined via its closest separable (or positive partial transpose) state σ. Recently, it has been shown how to find ρ provided that σ is given in a two-qubit system. In this article we study the reverse process, that is, how to find σ provided that ρ is given. It is shown that if ρ is of a Bell-diagonal, generalized Vedral-Plenio, or generalized Horodecki state, one can find σ from a geometrical point of view. This is possible due to the following two facts: (i) the Bloch vectors of ρ and σ are identical to each other; (ii) the correlation vector of σ can be computed from a crossing point between a minimal geometrical object, in which all separable states reside in the presence of Bloch vectors, and a straight line, which connects the point corresponding to the correlation vector of ρ and the nearest vertex of the maximal tetrahedron, where all two-qubit states reside. It is shown, however, that these properties are not maintained for the arbitrary two-qubit states.

DOI: 10.1103/PhysRevA.81.052325 PACS number(s): 03.67.Mn, 03.65.Ud, 42.50.Dv

I. INTRODUCTION

It is well known that entanglement of quantum states is an important physical resource in the context of the quantum information theories. It plays a crucial role in quantum teleportation [1], superdense coding [2], quantum cloning [3], quantum cryptography [4], and quantum computer technology [5,6].[1] Therefore, to understand how to quantify and how to characterize the entanglement for a given quantum state is a highly important physical task.

Many entanglement measures have been developed over past few years. Above all, in our opinion, the most important entanglement measure is a distillable entanglement [10], which quantifies how many maximally entangled states can be constructed from the copies of the given quantum state in the asymptotic region. The importance of the distillable entanglement arises from the fact that the entanglement is fragile when noises interfere with quantum information processing. The disadvantage of distillable entanglement is its calculational difficulty. In order to compute distillable entanglement analytically, we should find the optimal purification (or distillation) protocol. If this optimal protocol generates n maximally entangled states from m copies of the quantum state ρ, the distillable entanglement for ρ is given by[2]

$$D(\rho) = \lim_{m\to\infty} \frac{n}{m}. \tag{1}$$

However, finding an optimal purification protocol is a highly nontrivial task. It makes it difficult to compute distillable entanglement analytically.

Fortunately, the tight upper bound of distillable entanglement has been developed in Refs. [11,12]. In these references, the new entanglement measure called relative entropy of entanglement (REE) was introduced. It is defined as

$$E_R(\rho) = \min_{\sigma\in\mathcal{D}} S(\rho||\sigma), \tag{2}$$

where $\mathcal{D}$ is a set of separable states and $S(\rho||\sigma)$ is a quantum relative entropy; that is, $S(\rho||\sigma) = \mathrm{tr}(\rho\ln\rho - \rho\ln\sigma)$. It was shown in Ref. [12] that $E_R(\rho)$ is an upper bound of the distillable entanglement. Subsequently, Rains [13,14] has shown that

$$\tilde{E}_R(\rho) = \min_{\sigma\in\mathcal{D}_{\mathrm{PPT}}} S(\rho||\sigma), \tag{3}$$

where $\mathcal{D}_{PPT}$ is a set of positive partial transposition (PPT) states, is more tightly upper bound when ρ is an higher-dimensional bipartite state. Using the facts that the REE is an upper bound of the distillable entanglement and the Smolin state [15] is a bound entangled state, the distillable entanglement for the various Bell-state mixtures has been analytically computed [16–18]. In order to understand the distillable entanglement more deeply, therefore, it is important to develop various techniques for the explicit computation of the REE. Of course, regardless of the distillable entanglement, the development of a calculation technique for the REE itself is important for understanding the characterization of entanglement more profoundly. For last few years many properties of the REE were investigated [19]. Furthermore, the relation between the REE and other distance measures has been studied recently [20,21].

In this article we confine ourselves to the REE when ρ is a two-qubit state; that is, $\rho \in \mathcal{H}^2 \otimes \mathcal{H}^2$. Since there is no bound-entangled state in this case, $E_R(\rho)$ and $\tilde{E}_R(\rho)$ defined

[1]There are, however, several examples where entanglement does not play an important role in quantum computation. For example, the efficiency of Grover's search algorithm gets worsened if the initial state is an entangled one [7]. Another important example is a deterministic quantum computation with one pure qubit [8]. Other simple examples are presented in Ref. [9]. Therefore, one cannot conclude definitely that entanglement is essential for quantum computation.

[2]In Ref. [10], the distillable entanglement D is divided into D_1 and D_2 depending on one-way and two-way classical communications. Throughout this article we only consider the two-way classical communication.

in Eqs. (2) and (3) are same. Let σ^* be the closest separable state (CSS) of ρ. Then $E_R(\rho)$ is given by

$$E_R(\rho) = \min_{\sigma\in\mathcal{D}} S(\rho||\sigma) = S(\rho||\sigma^*). \tag{4}$$

When the CSS σ^* is explicitly given and is full rank, Ref. [22] has presented how to construct the set of the entangled states, whose CSS are σ^*. Let $|i\rangle$ and λ_i be eigenvectors and corresponding eigenvalues of σ^*. If σ^* is the CSS (hence, edge) state, then its partial transposition σ^Γ is rank deficient. Let $|\phi\rangle$ be the kernel of σ^Γ; that is,

$$\sigma^\Gamma|\phi\rangle = 0. \tag{5}$$

Then the set of the entangled states $\rho(x)$, whose CSSs are σ^*, is given by the following one-parameter family expression:

$$\begin{aligned} \rho(x) &= \sigma^* - xG(\sigma^*), \\ G(\sigma^*) &= \sum_{i,j} G_{ij}|i\rangle\langle i|(|\phi\rangle\langle\phi|)^\Gamma|j\rangle\langle j|, \end{aligned} \tag{6}$$

where $x \geqslant 0$ and

$$G_{ij} = \begin{cases} \lambda_i & \text{for } i = j, \\ \frac{\lambda_i - \lambda_j}{\ln\lambda_i - \ln\lambda_j} & \text{for } i \neq j. \end{cases} \tag{7}$$

When, however, the entangled state ρ is explicitly given, it is difficult to use Eq. (6) for finding its CSS. In other words, we have to find the reverse process of Ref. [22] in order to derive the closed formula of the REE for the arbitrary two-qubit state ρ, as Wootters [23] has done in the entanglement of formation. Unfortunately, it is still an unsolved problem [24].

In this article we explore the reverse process of Ref. [22]. We show that the reverse process of Ref. [22] is possible, at least for the Bell-diagonal, generalized Vedral-Plenio, and generalized Horodecki states. We present a method for finding the corresponding CSS systematically for these states by generalizing the geometrical method discussed by Horodecki in Ref. [25]. We also discuss why it is difficult to find the CSS for the arbitrary two-qubit mixed states from the geometrical point of view. The article is organized as follows. In Sec. II we show how to find the CSS for the Bell-diagonal states. In Sec. III we discuss how the geometrical objects presented in Ref. [25], such as tetrahedron $\mathcal{T}$ and octahedron $\mathcal{L}$, are deformed in the presence of the nonzero Bloch vectors. In Secs. IV and V we present a method for finding the corresponding CSS for the generalized Vedral-Plenio and generalized Horodecki states, respectively. In Sec. VI we discuss why it is a very difficult task to find the CSS for the arbitrary two-qubit states from the geometrical point of view. In Sec. VII a brief conclusion is given.

II. CSS FOR THE BELL-DIAGONAL STATES

In this section we show how to find the CSS when ρ is the Bell-diagonal state from the geometrical point of view. In fact, this problem was already solved in Ref. [12] long ago. The reason why we reconsider the same problem is to stress the geometrical analysis.

An arbitrary two-qubit state can be represented as follows:

$$\rho = \frac{1}{4}\left[I\otimes I + \boldsymbol{r}\cdot\boldsymbol{\sigma}\otimes I + I\otimes \boldsymbol{s}\cdot\boldsymbol{\sigma} + \sum_{m,n=1}^{3} g_{mn}\sigma_m\otimes\sigma_n\right], \tag{8}$$

where $\boldsymbol{r}$ and $\boldsymbol{s}$ are Bloch vectors and σ_i is a usual Pauli matrix. The coefficients g_{mn} form a real matrix and represent the interaction of the qubits. If state ρ is explicitly given, one can derive the Bloch vectors $\boldsymbol{r}$ and $\boldsymbol{s}$ and the correlation tensor g_{ij} as follows:

$$\boldsymbol{r} = \mathrm{tr}(\rho_A\boldsymbol{\sigma}), \quad \boldsymbol{s} = \mathrm{tr}(\rho_B\boldsymbol{\sigma}), \quad g_{ij} = \mathrm{tr}(\rho\sigma_i\otimes\sigma_j), \tag{9}$$

where $\rho_A = \mathrm{tr}_B\rho$ and $\rho_B = \mathrm{tr}_A\rho$. It is well known that an appropriate local unitary (LU) transformation of ρ can make g_{mn} diagonal (see appendix of Ref. [26]). Since entanglement is invariant under the LU transformation, it is in general sufficient to consider the case of diagonal g_{mn} for the discussion of entanglement. Thus, without loss of generality, one can express ρ as

$$\rho = \frac{1}{4}\left[I\otimes I + \boldsymbol{r}\cdot\boldsymbol{\sigma}\otimes I + I\otimes \boldsymbol{s}\cdot\boldsymbol{\sigma} + \sum_{n=1}^{3} g_n\sigma_n\otimes\sigma_n\right]. \tag{10}$$

If $\rho = |\beta_i\rangle\langle\beta_i|$, where

$$\begin{aligned} |\beta_1\rangle &= \frac{1}{\sqrt{2}}(|00\rangle + |11\rangle), \quad |\beta_2\rangle = \frac{1}{\sqrt{2}}(|00\rangle - |11\rangle), \\ |\beta_3\rangle &= \frac{1}{\sqrt{2}}(|01\rangle + |10\rangle), \quad |\beta_4\rangle = \frac{1}{\sqrt{2}}(|01\rangle - |10\rangle), \end{aligned} \tag{11}$$

it is easy to show that the corresponding Bloch vectors $\boldsymbol{r}$ and $\boldsymbol{s}$ are vanishing and the corresponding correlation tensor g_{mn} becomes

$$\begin{aligned} g_1 &= \mathrm{diag}(1,-1,1), \quad g_2 = \mathrm{diag}(-1,1,1), \\ g_3 &= \mathrm{diag}(1,1,-1), \quad g_4 = \mathrm{diag}(-1,-1,-1). \end{aligned} \tag{12}$$

If, therefore, ρ is the Bell-diagonal state, the Bloch vectors $\boldsymbol{r}$ and $\boldsymbol{s}$ are always null vectors.

Since we are considering on the diagonal case of the correlation tensor, we will regard, from now on, the tensor as a vector, whose components are equal to the diagonal elements. When $\boldsymbol{r} = \boldsymbol{s} = 0$, Horodecki has shown in Ref. [25] that the total two-qubit states belong to the tetrahedron $\mathcal{T}$ with vertices $v_1 = (1,-1,1)$, $v_2 = (-1,1,1)$, $v_3 = (1,1,-1)$, and $v_4 = (-1,-1,-1)$ in the correlation vector space. Reference [25] also has shown that the separable states (with $\boldsymbol{r} = \boldsymbol{s} = 0$) belong to the octahedron $\mathcal{L}$ with vertices $o_1^{(\pm)} = (\pm1,0,0)$, $o_2^{(\pm)} = (0,\pm1,0)$, and $o_3^{(\pm)} = (0,0,\pm1)$. This is pictorially represented in Fig. 1.

As Fig. 1 shows, the planes $(o_1^{(+)},o_2^{(-)},o_3^{(-)})$, $(o_1^{(+)},o_2^{(+)},o_3^{(+)})$, $(o_1^{(-)},o_2^{(-)},o_3^{(+)})$, and $(o_1^{(-)},o_2^{(+)},o_3^{(-)})$ are parts of the planes (v_1,v_3,v_4), (v_1,v_2,v_3), (v_1,v_2,v_4), and (v_2,v_3,v_4),

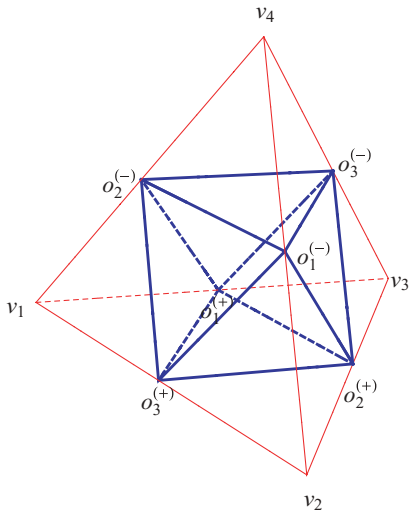

FIG. 1. (Color online) The total Bell-diagonal states belong to the tetrahedron (v_1,v_2,v_3,v_4) and the set of the separable states belong to the octahedron, whose vertices are $o_1^{\pm}$, $o_2^{\pm}$, and $o_3^{\pm}$. As this figure shows, the planes $(o_1^{(+)},o_2^{(-)},o_3^{(-)})$, $(o_1^{(+)},o_2^{(+)},o_3^{(+)})$, $(o_1^{(-)},o_2^{(-)},o_3^{(+)})$, and $(o_1^{(-)},o_2^{(+)},o_3^{(-)})$ are contained in the planes (v_1,v_3,v_4), (v_1,v_2,v_3), (v_1,v_2,v_4), and (v_2,v_3,v_4), respectively. Therefore, all entangled Bell-diagonal mixtures belong to the small four tetrahedra $(v_1,o_1^{(+)},o_2^{(-)},o_3^{(+)})$, $(v_2,o_1^{(-)},o_2^{(+)},o_3^{(+)})$, $(v_3,o_1^{(+)},o_2^{(+)},o_3^{(-)})$, and $(v_4,o_1^{(-)},o_2^{(-)},o_3^{(-)})$.

respectively.[3] Therefore, all entangled Bell-diagonal mixtures belong to the small four tetrahedra $(v_1,o_1^{(+)},o_2^{(-)},o_3^{(+)})$, $(v_2,o_1^{(-)},o_2^{(+)},o_3^{(+)})$, $(v_3,o_1^{(+)},o_2^{(+)},o_3^{(-)})$, and $(v_4,o_1^{(-)},o_2^{(-)},o_3^{(-)})$.

Now, we show how to perform the reverse process of Ref. [22] when ρ is an entangled Bell-diagonal state. This can be achieved by following two theorems.

Theorem 1. Every Bell state has infinite CSSs, which cover fully the nearest surface of the octahedron $\mathcal{L}$.

Proof. It is sufficient to prove this theorem when $\rho = |\beta_1\rangle\langle\beta_1|$. When $\rho = |\beta_i\rangle\langle\beta_i|$ $(i = 2,3,4)$, one can prove the theorem similarly.

Let σ be a following Bell-diagonal state:

$$\sigma = \frac{1}{4}\left[I\otimes I + \sum_{n=1}^{3} p_n \sigma_n \otimes \sigma_n\right], \tag{13}$$

with $\boldsymbol{p} = (x,y,z)$. Then it is easy to show that the spectral decomposition of σ is

$$\sigma = \frac{1+x-y+z}{4}|\beta_1\rangle\langle\beta_1| + \frac{1-x+y+z}{4}|\beta_2\rangle\langle\beta_2| + \frac{1+x+y-z}{4}|\beta_3\rangle\langle\beta_3| + \frac{1-x-y-z}{4}|\beta_4\rangle\langle\beta_4|. \tag{14}$$

[3]This statement can be confirmed by deriving the respective plane equations. The plane equations for (v_1,v_3,v_4), (v_1,v_2,v_3), (v_1,v_2,v_4), and (v_2,v_3,v_4) are $x-y-z=1$, $x+y+z=1$, $-x-y+z=1$, and $-x+y-z=1$, respectively. It is easy to show that these plane equations are the same planes with the planes $(o_1^{(+)},o_2^{(-)},o_3^{(-)})$, $(o_1^{(+)},o_2^{(+)},o_3^{(+)})$, $(o_1^{(-)},o_2^{(-)},o_3^{(+)})$, and $(o_1^{(-)},o_2^{(+)},o_3^{(-)})$, respectively.

The nearest surface of $\mathcal{L}$ from $\rho = |\beta_1\rangle\langle\beta_1|$ is $(o_1^{(+)},o_2^{(-)},o_3^{(+)})$, whose surface equation is $x-y+z=1$. If σ belongs to the surface $(o_1^{(+)},o_2^{(-)},o_3^{(+)})$, it is easy to show that $S(\rho||\sigma) = \ln 2$, which exactly coincides with the REE of the Bell states [11]. Therefore, σ on the surface $(o_1^{(+)},o_2^{(-)},o_3^{(+)})$ is the CSS of $|\beta_1\rangle\langle\beta_1|$.

Now, let us consider the case where σ belongs to another surface. For example, let us assume that σ belongs to the surface $(o_1^{(+)},o_2^{(+)},o_3^{(-)})$, whose surface equation is $x+y-z=1$. Then $S(\rho||\sigma)$ reduces to $\ln 2 - \ln x$, which is less than $\ln 2$ if $x \neq 1$. Therefore, σ on $(o_1^{(+)},o_2^{(+)},o_3^{(-)})$ is not the CSS of $|\beta_1\rangle\langle\beta_1|$. In same way, one can show that σ on $(o_1^{(-)},o_2^{(+)},o_3^{(+)})$ or $(o_1^{(-)},o_2^{(-)},o_3^{(-)})$ is not the CSS of $|\beta_1\rangle\langle\beta_1|$, which completes the proof.

Theorem 2. The CSS of the any Bell-diagonal state ρ corresponds to the crossing point between the nearest surface of $\mathcal{L}$ from ρ and the straight line ℓ, which connects ρ and the nearest vertex of $\mathcal{T}$ from ρ.

Proof. If σ is the CSS of ρ, the CSS of $\tilde{\rho} = x\rho + (1-x)\sigma$ is also σ [12]. Let ρ be $\rho = |\beta_1\rangle\langle\beta_1|$. Then Theorem 1 implies that σ can be any point on the surface $(o_1^{(+)},o_2^{(-)},o_3^{(+)})$. Let $\tilde{\rho}$ belong to the small tetrahedron $(v_1,o_1^{(+)},o_2^{(-)},o_3^{(+)})$. Note that $\tilde{\rho}$ corresponds to an internally dividing point of the line segment $\overline{\rho\sigma}$. Since Eq. (6) implies that the set of the entangled states which have the same CSSs should be represented by the straight line, the only possible σ as the CSS of $\tilde{\rho}$ is a crossing point between a line $\overline{\rho\tilde{\rho}}$ and the surface $(o_1^{(+)},o_2^{(-)},o_3^{(+)})$, which completes the proof for the Bell-diagonal states.

By making use of Theorem 2, one can always find the CSS σ if ρ is a Bell-diagonal state. Figure 2 shows how to find the CSS for the Bell-diagonal state. First, extend the line segment between ρ and the point corresponding to the nearest vertex of $\mathcal{T}$. Second, compute the coordinate of the crossing point between the line and the nearest surface of the octahedron $\mathcal{L}$. Finally, find the CSS which corresponds

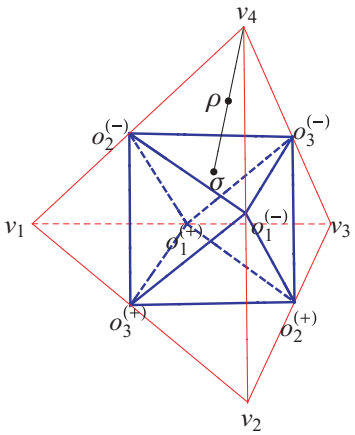

FIG. 2. (Color online) How to find the CSS for the Bell-diagonal state. First, extend the line segment between ρ and the point corresponding to the nearest vertex of $\mathcal{T}$. Second, compute the coordinate of the crossing point between the line and the nearest surface of the octahedron $\mathcal{L}$. Finally, find the CSS of ρ which corresponds to the crossing point.

TABLE I. Eigenvalues and eigenvectors of ρ in Eq. (15).

Eigenvalues of ρ	Eigenvectors of ρ
$\mu_\pm = \frac{1}{4}\{(1-q_3) \pm M_1\}$	$\lvert\mu_\pm\rangle = \frac{1}{\Lambda_\pm}[(q_1+q_2)\lvert 01\rangle - \{(r-s) \mp M_1\}\lvert 10\rangle]$
$\nu_\pm = \frac{1}{4}\{(1+q_3) \pm M_2\}$	$\lvert\nu_\pm\rangle = \frac{1}{\Delta_\pm}[(q_1-q_2)\lvert 00\rangle - \{(r+s) \mp M_2\}\lvert 11\rangle]$

to the crossing point. This completes the reverse process of Ref. [22].

III. GEOMETRICAL DEFORMATION OF $\mathcal{T}$ AND $\mathcal{L}$

When the Bloch vectors $\boldsymbol{r}$ and $\boldsymbol{s}$ are nonzero, the geometrical objects $\mathcal{T}$ and $\mathcal{L}$ should be deformed. In this section we will discuss how $\mathcal{T}$ and $\mathcal{L}$ are deformed. In order to perform the following analysis analytically, we consider in this article the case where $\boldsymbol{r}$ and $\boldsymbol{s}$ are parallel to each other. It is worthwhile noting that if $\boldsymbol{r}$ and $\boldsymbol{s}$ are x or y direction, one can make them to be z directional via the appropriate local-unitary transformation. For example, if they are x directional, $\rho' = (U\otimes U)\rho(U\otimes U)^\dagger$, where

$$U = \frac{1}{\sqrt{2}}\begin{pmatrix} 1 & 1 \\ -1 & 1 \end{pmatrix}$$

has z-directional Bloch vectors and its correlation vector changes from (g_1,g_2,g_3) to $(-g_3,g_2,g_1)$. Similarly, one can change the state with y-directional Bloch vectors into a state with z-directional Bloch vectors without altering the diagonal property of the correlation term.

For this reason it is reasonable to assume that the Bloch vectors are z directional by writing $\boldsymbol{r} = (0,0,r)$ and $\boldsymbol{s} = (0,0,s)$.[4] In this case the arbitrary two-qubit state ρ defined in Eq. (10) with $\boldsymbol{g} = (q_1,q_2,q_3)$ reduces to

$$\rho = \frac{1}{4}\begin{pmatrix} 1+r+s+q_3 & 0 & 0 & q_1-q_2 \\ 0 & 1+r-s-q_3 & q_1+q_2 & 0 \\ 0 & q_1+q_2 & 1-r+s-q_3 & 0 \\ q_1-q_2 & 0 & 0 & 1-r-s+q_3 \end{pmatrix}. \tag{15}$$

The eigenvalues and eigenvectors of ρ are summarized in Table I.

In Table I M_1, M_2, $\Lambda_\pm$, and $\Delta_\pm$ are given by

$$\begin{aligned} M_1 &= \sqrt{(r-s)^2+(q_1+q_2)^2}, \\ M_2 &= \sqrt{(r+s)^2+(q_1-q_2)^2}, \\ \Lambda_\pm &= \sqrt{\{(r-s)\mp M_1\}^2+(q_1+q_2)^2}, \\ \Delta_\pm &= \sqrt{\{(r+s)\mp M_2\}^2+(q_1-q_2)^2}. \end{aligned} \tag{16}$$

Then the deformation of $\mathcal{T}$ can be obtained from the positivity condition of ρ. Since deformation should be a set of the boundary states, the condition of the deformation becomes

$$\min(\mu_-,\nu_-) = 0. \tag{17}$$

One can make two surfaces by making use of Eq. (17). Each surface corresponds to $\min(\mu_-,\nu_-) = \mu_- = 0$ or $\min(\mu_-,\nu_-) = \nu_- = 0$. Gluing these surfaces together yields the deformation of $\mathcal{T}$.

In Fig. 3 we plot the deformation of $\mathcal{T}$ when $r = s = 0.3$ [Fig. 3(a)], $r = -s = 0.3$ [Fig. 3(b)], $r = s = 0.5$ [Fig. 3(c)], and $r = -s = 0.5$ [Fig. 3(d)]. For comparison, we plot $\mathcal{T}$ together. For convenience, we will denote the deformation of $\mathcal{T}$ with fixed r and s as $\mathcal{T}_{r,s}$. From Fig. 3 one can see that the deformation $\mathcal{T}_{r,s}$ has the following two characteristics. First is that the effect of the nonzero Bloch vectors is to shrink the geometrical object. The shrinking rate becomes larger with increasing $|r|$ and $|s|$. When $r = s$, the deformation is biased toward the (v_1,v_2) region. When, however, $r = -s$, the deformation is biased toward the (v_3,v_4) region. The shrinkage of $\mathcal{T}_{r,s}$ implies that the number of proper quantum states reduces with increasing $|r|$ and $|s|$ due to the constraint $\mathrm{tr}\rho^2 \leqslant 1$. The second characteristic of $\mathcal{T}_{r,s}$ is that it has a continuous smooth surface while $\mathcal{T}$ has sharp edges. This fact arises from the condition $\min(\mu_-,\nu_-) = 0$. When $r = s = 0$, this condition generates the four surface equations

$$\pm(q_1+q_2)+q_3 = 1, \quad \pm(q_1-q_2)-q_3 = 1, \tag{18}$$

each of which corresponds to the surface of $\mathcal{T}$. When, however, r and s are nonzero, these four equations reduce to the following two equations:

$$\begin{aligned} \sqrt{(r-s)^2+(q_1+q_2)^2}+q_3 &= 1, \\ \sqrt{(r+s)^2+(q_1-q_2)^2}-q_3 &= 1. \end{aligned} \tag{19}$$

This implies that the deformation $\mathcal{T}_{r,s}$ can be formed by attaching two smooth surfaces when $r \neq \pm s$.

[4]Even if $\boldsymbol{r}$ and $\boldsymbol{s}$ are not parallel to each other, one can make them to be z directional via an appropriate local-unitary transformation. In this case, however, the correlation term loses its diagonal property.

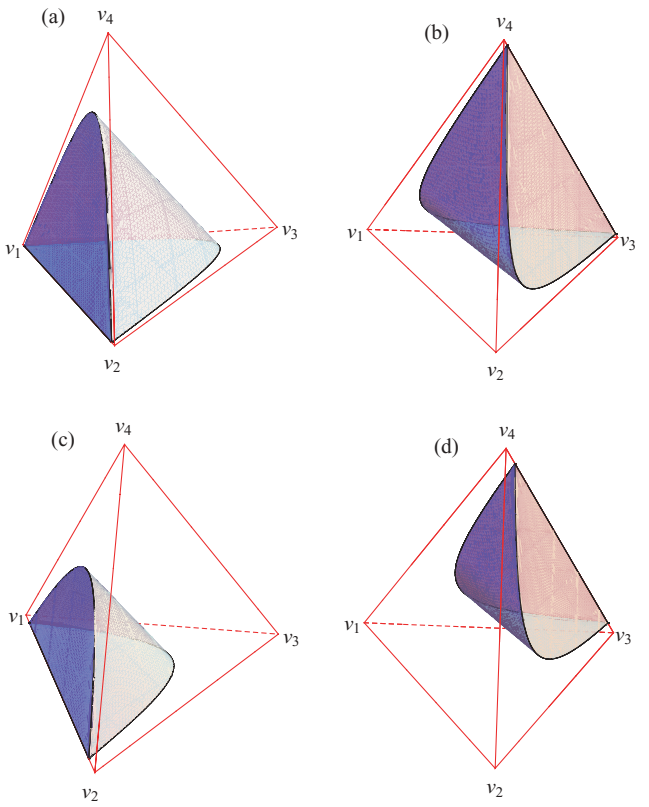

FIG. 3. (Color online) The deformation of $\mathcal{T}$ is plotted when $r = s = 0.3$ (a), $r = -s = 0.3$ (b), $r = s = 0.5$ (c), and $r = -s = 0.5$ (d). For comparison, we plot $\mathcal{T}$ together. The appearance of nonzero Bloch vectors generally shrinks the tetrahedron. The shrinking rate becomes larger with increasing norm of the Bloch vectors.

Now, we discuss the deformation of $\mathcal{L}$ when the Bloch vectors are $\boldsymbol{r} = (0,0,r)$ and $\boldsymbol{s} = (0,0,s)$. We will denote this deformation as $\mathcal{L}_{r,s}$. We assume that ρ in Eq. (15) is a separable state. In this case the PPT state of ρ, *say* ρ^Γ, should be positive. The eigenvalues and the corresponding eigenvectors of ρ^Γ are summarized in Table II.

In Table II M_1^Γ, M_2^Γ, $\Lambda_\pm^\Gamma$, and $\Delta_\pm^\Gamma$ are defined as

$$\begin{aligned} M_1^\Gamma &= M_1\big|_{q_2\to -q_2} = \sqrt{(r-s)^2+(q_1-q_2)^2}, \\ M_2^\Gamma &= M_2\big|_{q_2\to -q_2} = \sqrt{(r+s)^2+(q_1+q_2)^2}, \\ \Lambda_\pm^\Gamma &= \sqrt{\{(r-s)\mp M_1^\Gamma\}^2+(q_1-q_2)^2}, \\ \Delta_\pm^\Gamma &= \sqrt{\{(r+s)\mp M_2^\Gamma\}^2+(q_1+q_2)^2}. \end{aligned} \tag{20}$$

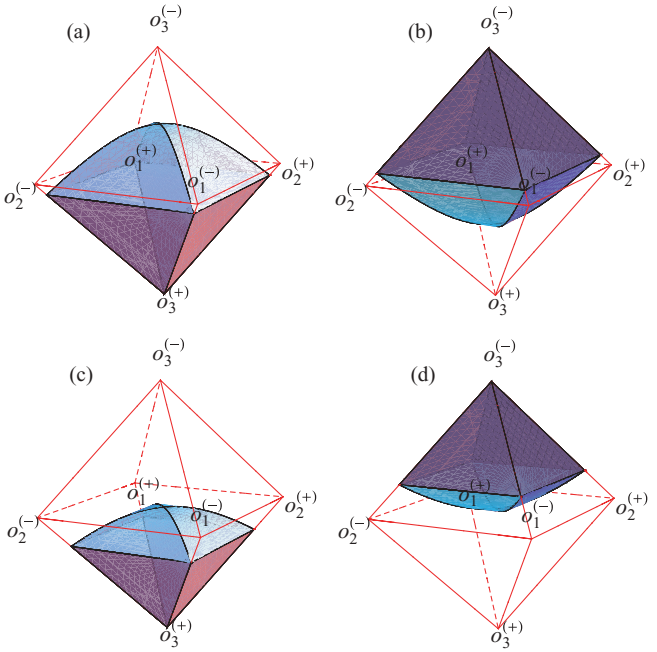

FIG. 4. (Color online) The deformation of $\mathcal{L}$ is plotted when $r = s = 0.3$ (a), $r = -s = 0.3$ (b), $r = s = 0.5$ (c), and $r = -s = 0.5$ (d). For comparison, we plot $\mathcal{L}$ together. The appearance of nonzero Bloch vectors generally shrinks the octahedron. The shrinking rate becomes larger with increasing norm of the Bloch vectors.

Then $\mathcal{L}_{r,s}$ can be obtained from the positivity condition of ρ^Γ. Since, furthermore, $\mathcal{L}_{r,s}$ should be a set of the edge states, the condition for the deformation of $\mathcal{L}$ reduces to

$$\min(\mu_-^\Gamma, \nu_-^\Gamma) = 0. \tag{21}$$

As the deformation of $\mathcal{T}$, Eq. (21) generates two surfaces, each of which corresponds to $\min(\mu_-^\Gamma,\nu_-^\Gamma) = \mu_-^\Gamma = 0$ or $\min(\mu_-^\Gamma,\nu_-^\Gamma) = \nu_-^\Gamma = 0$. Gluing these two surfaces, one can derive the deformation of $\mathcal{L}$.

In Fig. 4 we plot the deformation of $\mathcal{L}$ at $r = s = 0.3$ [Fig. 4(a)], $r = -s = 0.3$ [Fig. 4(b)], $r = s = 0.5$ [Fig. 4(c)], and $r = -s = 0.5$ [Fig. 4(d)]. For comparison, we plot $\mathcal{L}$ together. Like the deformation of $\mathcal{T}$, Fig. 4 indicates that the effect of the nonzero Bloch vectors is to shrink $\mathcal{L}$ toward a particular direction. Figure 4 also shows that the shrinking rate becomes larger and larger with increasing norm of the Bloch vectors. Like $\mathcal{T}_{r,s}$ again, the deformation of the octahedron $\mathcal{L}_{r,s}$ also has smooth surfaces while $\mathcal{L}$ has sharp edges.

IV. CSS FOR THE GENERALIZED VEDRAL-PLENIO STATES

In this section we show how to derive the CSS for the Vedral-Plenio (VP) states. The VP states are defined as mixture

TABLE II. Eigenvalues and eigenvectors of ρ^Γ.

Eigenvalues of ρ^Γ	Eigenvectors of ρ^Γ
$\mu_\pm^\Gamma = \frac{1}{4}\{(1-q_3)\pm M_1^\Gamma\}$	$\lvert\mu_\pm^\Gamma\rangle = \frac{1}{\Lambda_\pm^\Gamma}[(q_1-q_2)\lvert 01\rangle - \{(r-s)\mp M_1^\Gamma\}\lvert 10\rangle]$
$\nu_\pm^\Gamma = \frac{1}{4}\{(1+q_3)\pm M_2^\Gamma\}$	$\lvert\nu_\pm^\Gamma\rangle = \frac{1}{\Delta_\pm^\Gamma}[(q_1+q_2)\lvert 00\rangle - \{(r+s)\mp M_2^\Gamma\}\lvert 11\rangle]$

of one Bell state and separable states, which are not orthogonal to the Bell state. The most general example of the VP state is

$$\rho_{vp} = \lambda_1|\beta_1\rangle\langle\beta_1| + \lambda_2|00\rangle\langle 00| + \lambda_3|11\rangle\langle 11|, \tag{22}$$

where $|\beta_1\rangle = (1/\sqrt{2})(|00\rangle + |11\rangle)$ and $\lambda_1 + \lambda_2 + \lambda_3 = 1$.

Let the arbitrary VP state be

$$\rho_{vp} = \frac{1}{4}\Bigg[I \otimes I + \boldsymbol{r}_{\rm vp}\cdot\boldsymbol{\sigma}\otimes I + I\otimes \boldsymbol{s}_{\rm vp}\cdot\boldsymbol{\sigma} + \sum_{n=1}^{3}(\boldsymbol{t}_{\rm vp})_n\sigma_n\otimes\sigma_n\Bigg] \tag{23}$$

and its CSS be

$$\pi_{vp} = \frac{1}{4}\Bigg[I \otimes I + \boldsymbol{u}_{\rm vp}\cdot\boldsymbol{\sigma}\otimes I + I\otimes \boldsymbol{v}_{\rm vp}\cdot\boldsymbol{\sigma} + \sum_{n=1}^{3}(\boldsymbol{\tau}_{\rm vp})_n\sigma_n\otimes\sigma_n\Bigg]. \tag{24}$$

The following theorem shows how to compute $\boldsymbol{u}_{\rm vp}$, $\boldsymbol{v}_{\rm vp}$, and $\boldsymbol{\tau}_{\rm vp}$ from $\rho_{\rm vp}$.

Theorem 3. If $\pi_{\rm vp}$ is the CSS of $\rho_{\rm vp}$, $\boldsymbol{u}_{\rm vp} = \boldsymbol{r}_{\rm vp}$ and $\boldsymbol{v}_{\rm vp} = \boldsymbol{s}_{\rm vp}$. Let ℓ be a straight line which connects $\boldsymbol{t}_{\rm vp}$ and the nearest vertex of $\mathcal{T}$. Then $\boldsymbol{\tau}_{\rm vp}$ is a crossing point between ℓ and $\mathcal{L}_{r,s}$.

Proof. We prove this theorem using following procedure. First, we assume that this theorem is correct. Then, following this theorem, one can derive the trial CSS of $\rho_{\rm vp}$. Next, by making use of Eq. (6) we show that this trial CSS is a really the CSS of $\rho_{\rm vp}$.

Since other VP states can be derived from Eq. (22) by local-unitary (LU) transformation, it is sufficient to show that the CSS of $\rho_{\rm vp}$ in Eq. (22) satisfies this theorem. The other case can be proven similarly. For $\rho_{\rm vp}$ in Eq. (22) $\boldsymbol{r}_{\rm vp}$, $\boldsymbol{s}_{\rm vp}$, and $\boldsymbol{t}_{\rm vp}$ become $\boldsymbol{r}_{\rm vp} = (0,0,r)$, $\boldsymbol{s}_{\rm vp} = (0,0,s)$, and $\boldsymbol{t}_{\rm vp} = (t_1,t_2,t_3)$, where

$$r = s = \lambda_2 - \lambda_3, \quad t_1 = -t_2 = \lambda_1, \quad t_3 = 1. \tag{25}$$

Then a point $P = (q_1,q_2,q_3)$ on the line ℓ satisfies $q_2 = -q_1$ and $q_3 = 1$. If the point $P = (q_1,q_2,q_3)$ is a crossing point between ℓ and $\mathcal{L}_{r,s}$, the corresponding separable state satisfies

$$\mu_-^\Gamma = -\tfrac{1}{2}|q_1|, \quad \nu_-^\Gamma = \tfrac{1}{2}(1 - |\lambda_2 - \lambda_3|), \tag{26}$$

where μ_-^Γ and ν_-^Γ are defined in Table II. Therefore, the CSS condition (21) implies $q_1 = 0$, which results in $\boldsymbol{\tau}_{\rm vp} = (0,0,1)$. If, therefore, this theorem is correct, the CSS of $\rho_{\rm vp}$ is

$$\pi_{\rm vp} = \frac{1}{4}\left[I\otimes I + (\lambda_2-\lambda_3)(\sigma_3\otimes I + I\otimes\sigma_3) + \sigma_3\otimes\sigma_3\right] = \begin{pmatrix} \frac{\lambda_1}{2}+\lambda_2 & 0 & 0 & 0 \\ 0 & 0 & 0 & 0 \\ 0 & 0 & 0 & 0 \\ 0 & 0 & 0 & \frac{\lambda_1}{2}+\lambda_3 \end{pmatrix}. \tag{27}$$

In order to show that $\pi_{\rm vp}$ in Eq. (27) is really the CSS of $\rho_{\rm vp}$, it is convenient to define another edge state,

$$\tilde{\pi}_{\rm vp} = (\mathbb{1}\otimes\sigma_x)\pi_{\rm vp}(\mathbb{1}\otimes\sigma_x)^\dagger = \begin{pmatrix} \epsilon & 0 & 0 & 0 \\ 0 & \frac{\lambda_1}{2}+\lambda_2 & \epsilon & 0 \\ 0 & \epsilon & \frac{\lambda_1}{2}+\lambda_3 & 0 \\ 0 & 0 & 0 & \epsilon \end{pmatrix}, \tag{28}$$

where the infinitesimal positive parameter ϵ is introduced for convenience. This parameter will be taken to be zero after calculation.

Let us define an edge state

$$\sigma_Z = \begin{pmatrix} R_1 & 0 & 0 & 0 \\ 0 & R_2 & Y & 0 \\ 0 & Y & R_3 & 0 \\ 0 & 0 & 0 & R_4 \end{pmatrix}, \tag{29}$$

with $Y = \sqrt{R_1R_4}$ and $R_2R_3 \geqslant R_1R_4$. Then, by making use of Eq. (6), Ref. [22] has shown that the set of the entangled states which have σ_Z as the CSS is represented as

$$\rho_Z(x) = \begin{pmatrix} R_1 - x\bar{R}_1 & 0 & 0 & 0 \\ 0 & R_2 - x\bar{R}_2 & Y - x\bar{Y} & 0 \\ 0 & Y - x\bar{Y} & R_3 - x\bar{R}_3 & 0 \\ 0 & 0 & 0 & R_4 - x\bar{R}_4 \end{pmatrix}, \tag{30}$$

where $x \geqslant 0$ and[5]

$$\begin{aligned} \bar{R}_1 = \bar{R}_4 &= \frac{Y^2}{R_1+R_4}, \\ \bar{R}_2 &= 2Y^2d[(R_2-R_3)(R_2L-z) + 2Y^2L], \\ \bar{R}_3 &= -2\bar{R}_1 - \bar{R}_2, \\ \bar{Y} &= Yd[2Y^2(R_2+R_3)L + (R_2-R_3)^2z]. \end{aligned} \tag{31}$$

In Eq. (31) we define

$$z = \sqrt{(R_2-R_3)^2 + 4R_1R_4}, \quad L = \ln\left[\frac{(R_2+R_3)+z}{(R_2+R_3)-z}\right], \quad d = -\frac{1}{(R_1+R_4)z^2L}. \tag{32}$$

Now, we identify σ_Z with $\tilde{\pi}_{\rm vp}$ by putting $R_1 = R_4 = Y = \epsilon$, $R_2 = \lambda_1/2 + \lambda_2$, and $R_3 = \lambda_1/2 + \lambda_3$. Then it is straightforward to compute $\bar{R}_1$, $\bar{R}_2$, $\bar{R}_3$, $\bar{R}_4$, and $\bar{Y}$. After taking the $\epsilon \to 0$ limit, one can show $\bar{R}_1 = \bar{R}_2 = \bar{R}_3 = \bar{R}_4 = 0$ and

[5]We corrected the sign mistake of Ref. [22].

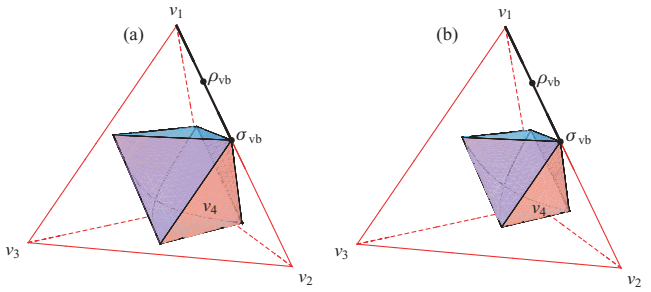

FIG. 5. (Color online) How to find the CSS for the VP states. Panels (a) and (b) correspond to $r = s = 0.3$ and $r = s = 0.5$, respectively. To find a CSS, make a straight line ℓ first, which connects the nearest vertex of $\mathcal{T}$ and a point $\boldsymbol{t}_{\rm vp}$. Second, compute the coordinate for the intersection point between ℓ and $\mathcal{L}_{r,s}$. Third, identify the crossing point with $\boldsymbol{\tau}_{\rm vp}$. Keeping $\boldsymbol{u}_{\rm vp} = \boldsymbol{r}_{\rm vp}$ and $\boldsymbol{v}_{\rm vp} = \boldsymbol{s}_{\rm vp}$, one can find the CSS of the VP state.

$\bar{Y} = -|\lambda_2 - \lambda_3|/2L$, where

$$L = \ln \frac{1 + |\lambda_2 - \lambda_3|}{1 - |\lambda_2 - \lambda_3|} \geqslant 0. \tag{33}$$

Therefore, the set of the entangled states which have $\tilde{\pi}_{\rm vp}$ as the CSS can be represented by

$$\tilde{\rho}_Z(x) = \begin{pmatrix} 0 & 0 & 0 & 0 \\ 0 & \frac{\lambda_1}{2} + \lambda_2 & x\frac{|\lambda_2 - \lambda_3|}{2L} & 0 \\ 0 & x\frac{|\lambda_2 - \lambda_3|}{2L} & \frac{\lambda_1}{2} + \lambda_3 & 0 \\ 0 & 0 & 0 & 0 \end{pmatrix}. \tag{34}$$

Finally, the set of the entangled states which have $\pi_{\rm vp}$ as the CSS can be derived by taking the inverse LU transformation; that is,

$$\rho_Z(x) = (\mathbb{1} \otimes \sigma_x)^\dagger \tilde{\rho}_Z(x)(\mathbb{1} \otimes \sigma_x). \tag{35}$$

It is easy to show that $\rho_Z(x)$ reduces to $\rho_{\rm vp}$ in Eq. (22) when $x = x_{\rm vp} = \lambda_1 L/|\lambda_2 - \lambda_3| \geqslant 0$, which completes the proof.

Figure 5 shows how to find the CSS for the VP state geometrically when $r = s = 0.3$ [Fig. 5(a)] and $r = s = 0.5$ [Fig. 5(b)]. Figure 5 indicates that the generalized VP states are on the edges of $\mathcal{T}$. First we make a line, which connects the nearest vertex of $\mathcal{T}$ and $\rho_{\rm vp}$. Then we compute the coordinate of the crossing point $\boldsymbol{\tau}$ between the line and $\mathcal{L}_{r,s}$. Finally, the CSS $\pi_{\rm vp}$ of $\rho_{\rm vp}$ can be computed by Eq. (24), keeping the Bloch vectors.

V. CSS FOR THE GENERALIZED HORODECKI STATES

In this section we discuss how to derive the CSS of the generalized Horodecki states. The Horodecki states are defined as a mixture of one Bell state and separable states, which are orthogonal to the Bell state. The most general example of the VP state is

$$\rho_H = \lambda_1 |\beta_1\rangle\langle\beta_1| + \lambda_2 |01\rangle\langle 01| + \lambda_3 |10\rangle\langle 10|, \tag{36}$$

with $\lambda_1 + \lambda_2 + \lambda_3 = 1$. By contrast with the VP state, the Horodecki state (36) is separable when $\lambda_1^2 \leqslant 4\lambda_2\lambda_3$. This can be easily understood by computing the concurrence of ρ_H, which is

$$\mathcal{C}(\rho_H) = \begin{cases} \lambda_1 - 2\sqrt{\lambda_2\lambda_3} & \text{if } \lambda_1 \geqslant 2\sqrt{\lambda_2\lambda_3}, \\ 0 & \text{if } \lambda_1 \leqslant 2\sqrt{\lambda_2\lambda_3}. \end{cases} \tag{37}$$

Thus, $\mathcal{C}(\rho_H)$ becomes zero when $\lambda_1^2 \leqslant 4\lambda_2\lambda_3$, which indicates that ρ_H is separable in this region.

Let the arbitrary Horodecki state be

$$\rho_H = \frac{1}{4}\Big[I \otimes I + \boldsymbol{r}_H \cdot \boldsymbol{\sigma} \otimes I + I \otimes \boldsymbol{s}_H \cdot \boldsymbol{\sigma} + \sum_{n=1}^{3} (t_H)_n \sigma_n \otimes \sigma_n \Big] \tag{38}$$

and its CSS be

$$\pi_H = \frac{1}{4}\Big[I \otimes I + \boldsymbol{u}_H \cdot \boldsymbol{\sigma} \otimes I + I \otimes \boldsymbol{v}_H \cdot \boldsymbol{\sigma} + \sum_{n=1}^{3} (\tau_H)_n \sigma_n \otimes \sigma_n \Big]. \tag{39}$$

The following theorem shows how to compute $\boldsymbol{u}_H$, $\boldsymbol{v}_H$, and $\boldsymbol{\tau}_H$ from ρ_H.

Theorem 4. If π_H is a CSS of ρ_H, $\boldsymbol{u}_H = \boldsymbol{r}_H$ and $\boldsymbol{v}_H = \boldsymbol{s}_H$. Let ℓ be a straight line which connects $\boldsymbol{t}_H$ and the nearest vertex of $\mathcal{T}$. Then $\boldsymbol{\tau}_H$ is the nearest crossing point between ℓ and $\mathcal{L}_{r,s}$.

Proof. We will prove this theorem by following the same procedure as Theorem 3. Since other Horodecki states can be derived from ρ_H in Eq. (36) by LU transformation, it is sufficient to show that the CSS of Eq. (36) satisfies this theorem. By identifying Eq. (36) with Eq. (38) one can easily show that $\boldsymbol{r}_H, \boldsymbol{s}_H$, and $\boldsymbol{t}_H$ become $\boldsymbol{r}_H = (0,0,r)$, $\boldsymbol{s}_H = (0,0,s)$, and $\boldsymbol{t}_H = (t_1,t_2,t_3)$, where

$$r = -s = \lambda_2 - \lambda_3, \quad t_1 = -t_2 = \lambda_1, \quad t_3 = 2\lambda_1 - 1. \tag{40}$$

Then a point $P(q_1,q_2,q_3)$ on the line ℓ satisfies $q_2 = q_1$ and $q_3 = 2q_1 - 1$.

Let the point P be the crossing point between ℓ and $\mathcal{L}_{r,s}$. Then μ_-^Γ and ν_-^Γ for the state corresponding to the point P are given by

$$\mu_-^\Gamma = \frac{1}{2}\Big[(1 - q_1) - \sqrt{q_1^2 + (\lambda_2 - \lambda_3)^2}\Big], \quad \nu_-^\Gamma = \frac{q_1}{2}. \tag{41}$$

Therefore, the CSS condition $\min(\mu_-^\Gamma, \nu_-^\Gamma) = 0$ gives two solutions, $P_1 = (q_1, -q_1, 2q_1 - 1)$ and $P_2 = (0,0,-1)$, where

$$q_1 = \tfrac{1}{2}(\lambda_1 + 2\lambda_2)(\lambda_1 + 2\lambda_3). \tag{42}$$

Since we have to choose the nearest point from $\boldsymbol{t}_H$, the solution we want is the former. Therefore, $\boldsymbol{\tau}_H$ becomes $(q_1, -q_1, 2q_1 - 1)$. Then Theorem 4 claims that the CSS of ρ_H is

$$\pi_H = \frac{1}{4}[I\otimes I + (\lambda_2-\lambda_3)\{\sigma_3\otimes I - I\otimes\sigma_3\} + q_1\sigma_1\otimes\sigma_1 - q_1\sigma_2\otimes\sigma_2 + (2q-1)\sigma_3\otimes\sigma_3]$$
$$= \frac{1}{4}\begin{pmatrix} (\lambda_1+2\lambda_2)(\lambda_1+2\lambda_3) & 0 & 0 & (\lambda_1+2\lambda_2)(\lambda_1+2\lambda_3) \\ 0 & (\lambda_1+2\lambda_2)^2 & 0 & 0 \\ 0 & 0 & (\lambda_1+2\lambda_3)^2 & 0 \\ (\lambda_1+2\lambda_2)(\lambda_1+2\lambda_3) & 0 & 0 & (\lambda_1+2\lambda_2)(\lambda_1+2\lambda_3) \end{pmatrix}. \quad (43)$$

Now, we will show that π_H in Eq. (43) is really the CSS of ρ_H by making use of Eq. (6). In order to show this, we define $\tilde{\pi}_H = (\mathbb{1}\otimes\sigma_x)\pi_H(\mathbb{1}\otimes\sigma_x)^\dagger$. Then by making use of Eqs. (29) and (30) it is straightforward to find a set of the entangled quantum states $\tilde{\rho}(x)$, whose CSSs are $\tilde{\pi}_H$. After taking the inverse LU transformation, one can derive $\rho(x) = (\mathbb{1}\otimes\sigma_x)^\dagger\tilde{\rho}(x)(\mathbb{1}\otimes\sigma_x)$. The expression of $\rho(x)$ is

$$\rho(x) = \begin{pmatrix} Y+x\eta & 0 & 0 & Y+x\eta \\ 0 & R_1-x\eta & 0 & 0 \\ 0 & 0 & R_4-x\eta & 0 \\ Y+x\eta & 0 & 0 & Y+x\eta \end{pmatrix}, \quad (44)$$

where $x \geqslant 0$ and

$$R_1 = \frac{1}{4}(\lambda_1+2\lambda_2)^2, \quad R_4 = \frac{1}{4}(\lambda_1+2\lambda_3)^2,$$
$$Y = \frac{1}{4}(\lambda_1+2\lambda_2)(\lambda_1+2\lambda_3), \quad \eta = \frac{Y^2}{R_1+R_4}. \quad (45)$$

When

$$x = x_H = \frac{1}{\eta}\left(\frac{\lambda_1}{2} - Y\right), \quad (46)$$

$\rho(x)$ reduces to ρ_H in Eq. (36). It is easy to prove that $x_H \geqslant 0$ if $\lambda_1^2 \geqslant 4\lambda_2\lambda_3$, which is an entangled condition for ρ_H. Therefore, Theorem 4 is completely proved.

Figure 6 shows how to find the CSS for the generalized Horodecki state ρ_H when $r = -s = 0.3$ [Fig. 6(a)] and $r = -s = 0.5$ [Fig. 6(b)]. If ρ_H is explicitly given, compute $\boldsymbol{r}_H, \boldsymbol{s}_H$, and $\boldsymbol{t}_H$. Then make a straight line which connects a point $\boldsymbol{t}_H$ and the nearest vertex of $\mathcal{T}$. Find the crossing points between the line and $\mathcal{L}_{r,s}$. As Fig. 3 shows, there are two intersection points P_1 and P_2 for the Horodecki states. This is why the CSS condition $\min(\mu_-^\Gamma, \nu_-^\Gamma) = 0$ gives two different solutions. Using the nearest crossing point (P_1 in Fig. 6), one can derive $\boldsymbol{\tau}_H$ straightforwardly. Finally, using Eq. (39) with imposing $\boldsymbol{u}_H = \boldsymbol{r}_H$ and $\boldsymbol{v}_H = \boldsymbol{s}_H$, one can derive π_H, the CSS of ρ_H.

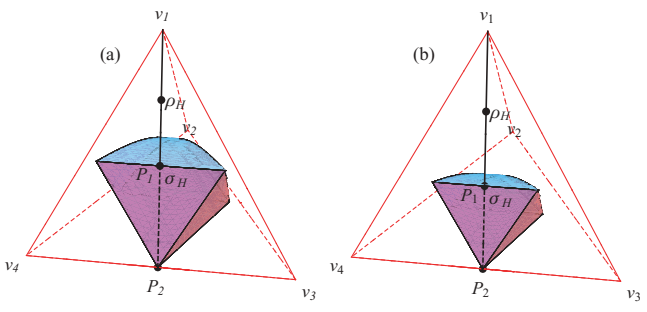

FIG. 6. (Color online) How to find the CSS for the generalized Horodecki states. Panels (a) and (b) correspond to $r = -s = 0.3$ and $r = -s = 0.5$ respectively. In order to find the CSS, make a straight line ℓ first, which connects the nearest vertex of $\mathcal{T}$ and a point $\boldsymbol{t}_H$. Second, compute the coordinate for the nearest crossing point between ℓ and $\mathcal{L}_{r,s}$. Third, identify the crossing point with $\boldsymbol{\tau}_H$. Keeping $\boldsymbol{u}_H = \boldsymbol{r}_H$ and $\boldsymbol{v}_H = \boldsymbol{s}_H$, one can find the CSS of the Horodecki state.

VI. DIFFICULTIES IN FINDING THE CSS FOR ARBITRARY STATES

In the previous sections we have shown how to find the CSS for the Bell-diagonal, generalized VP, and generalized Horodecki states. In fact, it is possible to find the CSS because those states exhibit the following features. Let $\boldsymbol{r}$, $\boldsymbol{s}$, and $\boldsymbol{t}$ be Bloch and correlation vectors of those states. Let $\boldsymbol{u}$, $\boldsymbol{v}$, and $\boldsymbol{\tau}$ be Bloch and correlation vectors for the corresponding CSS of those states. Then the features are as follows.

(i) $\boldsymbol{u} = \boldsymbol{r}$ and $\boldsymbol{v} = \boldsymbol{s}$.

(ii) $\boldsymbol{\tau}$ can be computed from the crossing point between the straight line ℓ and the surface for a set of the separable states $\mathcal{L}_{r,s}$.

However, such simple but nice features are not maintained for the general mixtures. For example, let us consider the comparatively simple model introduced in Eqs. (29) and (30). It is straightforward to show that the first property, that is, $\boldsymbol{u} = \boldsymbol{r}$ and $\boldsymbol{v} = \boldsymbol{s}$, is not maintained unless $R_2 = R_3$.[6] In order to find the CSS for the arbitrary states, therefore, we have to find the explicit relations between $(\boldsymbol{r},\boldsymbol{s})$ and $(\boldsymbol{u},\boldsymbol{v})$. As far as we know, still this is an unsolved problem.

In addition, one can show that the second property is not maintained too for the general mixtures. Using Eq. (6) we plot the $\boldsymbol{\tau}$ (correlation vector of the CSS)-dependence of $\boldsymbol{t}$ (correlation vector of the entangled state) with varying parameter x when $\min(\mu_-^\Gamma, \nu_-^\Gamma) = \nu_-^\Gamma = 0$. Since similar behavior arises when $\min(\mu_-^\Gamma, \nu_-^\Gamma) = \mu_-^\Gamma = 0$, we have not included this case in Fig. 7. The four panels in Fig. 7 correspond to, respectively, $r = s = 0.3$ [Fig. 7(a)], $r = -s = 0.3$ [Fig. 7(b)], $r = s = 0.5$ [Fig. 7(c)], and $r = -s = 0.5$ [Fig. 7(d)]. For convenience, we plot $\mathcal{T}$ and $\mathcal{L}_{r,s}$ together in each figure. Each line in Fig. 7 represents a set of $\boldsymbol{t}$, whose CSS has the same $\boldsymbol{\tau}$. As Fig. 7 exhibits, not all lines pass one of the vertices of $\mathcal{T}$. This fact

[6]When $R_2 = R_3$, one can show $[\rho_Z(x), \sigma_Z] = 0$. Therefore, $E_R[\rho_Z(x)\otimes\tilde{\rho}] = E_R[\rho_Z(x)] + E_R(\tilde{\rho})$ for all two-qubit mixtures $\tilde{\rho}$ [14].

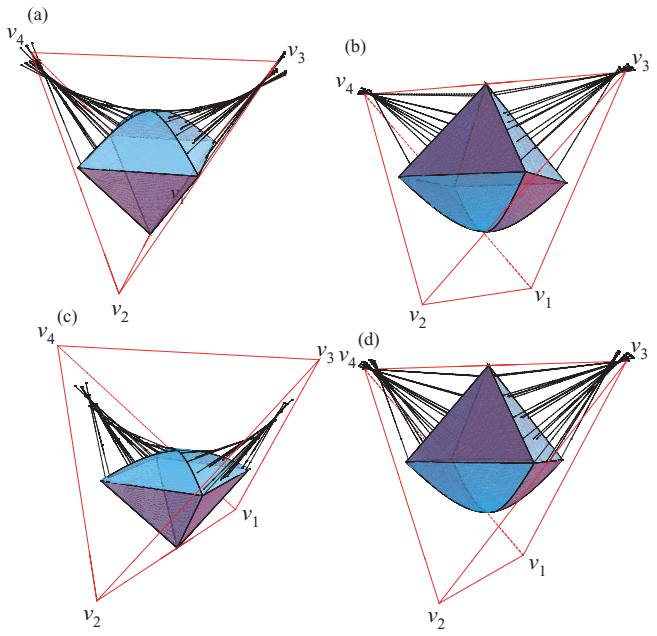

FIG. 7. (Color online) Illustration of how property (ii) is not maintained for the arbitrary two-qubit states. The four panels correspond to $r = s = 0.3$ (a), $r = -s = 0.3$ (b), $r = s = 0.5$ (c), and $r = -s = 0.5$ (d). For convenience, we plot $\mathcal{T}$ and $\mathcal{L}_{r,s}$ together in each figure. Each line represents a set of $\boldsymbol{t}$ whose CSS has the same $\boldsymbol{\tau}$. Not all lines pass one of the vertices of $\mathcal{T}$. This fact indicates that property (ii) is not maintained for the general mixtures.

indicates that, unfortunately, property (ii) is not maintained for the arbitrary states.

The nonmaintenance of property (ii) can be proved on an analytical ground by making use of the simpler model. Let us consider σ_Z in Eq. (29) and $\rho_Z(x)$ in Eq. (30). Then the Bloch vectors $\boldsymbol{r}$, $\boldsymbol{s}$ and the correlation vector $\boldsymbol{t}$ of $\rho_Z(x)$ are $\boldsymbol{r} = (0,0,r)$, $\boldsymbol{s} = (0,0,s)$, and $\boldsymbol{t} = (t_1,t_2,t_3)$, where

$$\begin{aligned} r &= (R_1 + R_2 - R_3 - R_4) - x(\bar{R}_2 - \bar{R}_3), \\ s &= (R_1 - R_2 + R_3 - R_4) + x(\bar{R}_2 - \bar{R}_3), \\ t_1 = t_2 &= 2Y - 2x\bar{Y}, \quad t_3 = (R_1 - R_2 - R_3 + R_4) - 4x\bar{R}_1. \end{aligned} \tag{47}$$

Of course, if we take the $x \to 0$ limit in Eq. (47), the corresponding quantities are the Bloch vectors and the correlation vector of σ_Z. Now, let us consider another state π_Z, which can be obtained from σ_Z by changing $Y \to Y'$ and $R_i \to R_i'$ $(i = 1,\ldots,4)$. In order to ensure that π_Z is the CSS, we require $Y' = \sqrt{R_1' R_4'}$ and $R_2' R_3' \geqslant R_1' R_4'$. Then the set of the entangled states $\xi_Z(x')$, whose CSSs are π_Z, can be obtained from $\rho_Z(x)$ by changing $Y \to Y'$, $R_i \to R_i'$ $(i = 1,\ldots,4)$, and $x \to x'$. Thus, Bloch vectors $\boldsymbol{r}'$, $\boldsymbol{s}'$ and correlation vector $\boldsymbol{t}'$ of $\xi_Z(x')$ are $\boldsymbol{r}' = (0,0,r')$, $\boldsymbol{s}' = (0,0,s')$, and $\boldsymbol{t}' = (t_1',t_2',t_3')$, where

$$\begin{aligned} r' &= (R_1' + R_2' - R_3' - R_4') - x'(\bar{R}_2' - \bar{R}_3'), \\ s' &= (R_1' - R_2' + R_3' - R_4') + x'(\bar{R}_2' - \bar{R}_3'), \\ t_1' = t_2' &= 2Y' - 2x'\bar{Y}', \quad t_3' = (R_1' - R_2' - R_3' + R_4') - 4x'\bar{R}_1'. \end{aligned} \tag{48}$$

Then it is straightforward to show that the condition $\boldsymbol{t} = \boldsymbol{t}'$ imposes

$$\begin{aligned} x &= \frac{\bar{Y}'(\tilde{r} - \tilde{r}') - 4(Y - Y')\bar{R}_1'}{4(\bar{Y}'\bar{R}_1 - \bar{Y}\bar{R}_1')}, \\ x' &= \frac{\bar{Y}(\tilde{r} - \tilde{r}') - 4(Y - Y')\bar{R}_1}{4(\bar{Y}'\bar{R}_1 - \bar{Y}\bar{R}_1')}, \end{aligned} \tag{49}$$

where $\tilde{r} = R_1 - R_2 - R_3 + R_4$ and $\tilde{r}' = R_1' - R_2' - R_3' + R_4'$. Thus, one can compute the crossing point $\boldsymbol{t} = \boldsymbol{t}' = (\mu_1,\mu_2,\mu_3)$, where μ_i becomes

$$\begin{aligned} \mu_1 = \mu_2 &= \frac{4(Y\bar{Y}'\bar{R}_1 - Y'\bar{Y}\bar{R}_1') - \bar{Y}\bar{Y}'(\tilde{r} - \tilde{r}')}{2(\bar{Y}'\bar{R}_1 - \bar{Y}\bar{R}_1')}, \\ \mu_3 &= \frac{4(Y - Y')\bar{R}_1\bar{R}_1' - (\tilde{r}\bar{Y}\bar{R}_1' - \tilde{r}'\bar{Y}'\bar{R}_1)}{\bar{Y}'\bar{R}_1 - \bar{Y}\bar{R}_1'}. \end{aligned} \tag{50}$$

As a special case, we consider the Bell-diagonal case by letting $R_1 = R_4 = Y = 2\bar{R}_1 = 2\bar{R}_4 = -2\bar{R}_2 = -2\bar{R}_3 = a$, $R_2 = R_3 = -2\bar{Y} = b$, $R_1' = R_4' = Y' = 2\bar{R}_1' = 2\bar{R}_4' = -2\bar{R}_2' = -2\bar{R}_3' = a'$, and $R_2' = R_3' = -2\bar{Y}' = b'$. Of course, one can show directly that $\rho_Z(x)$ and $\xi_Z(x')$ are really Bell-diagonal states. Using the normalization conditions $2(a + b) = 2(a' + b') = 1$, it is easy to verify that the crossing point (μ_1,μ_2,μ_3) is simply $\mu_1 = \mu_2 = 1$ and $\mu_3 = -1$, which is one of the vertices of $\mathcal{T}$. It is worthwhile noting that the crossing point is independent of the particular choice of Bell-diagonal states $\rho_Z(x)$ and $\xi_Z(x')$. This fact implies that all straight lines, which connect $\boldsymbol{\tau}$ and $\boldsymbol{t}$, pass one of the vertices of $\mathcal{T}$, which is consistent with Theorem 2.

However, for the arbitrary mixtures Eq. (50) implies that the crossing point (μ_1,μ_2,μ_3) is dependent on the choice of the entangled states $\rho_Z(x)$ and $\xi_Z(x')$. This is why property (ii), which holds for the Bell-diagonal, generalized VP, and generalized Horodecki states, does not hold for the arbitrary mixture as Fig. 7 has indicated. Therefore, in order to derive the closed formula of $E_R(\rho)$ for the arbitrary two-qubit mixtures ρ, we have to understand how property (ii) is modified when $\boldsymbol{r}$, $\boldsymbol{s}$, and $\boldsymbol{t}$ are arbitrary. Unfortunately, this is still an unsolved problem too.

VII. CONCLUSION

In this article we have considered how to find the CSS in the two-qubit system from the geometrical point of view. Of course, one can straightforwardly compute the REE of the state ρ if its CSS is found. Therefore, it is important to develop a technique for finding a CSS to overcome the calculational difficulty of the REE. Furthermore, since the REE is a tight upper bound of the distillable entanglement, finding the CSS is also important for understanding the nature of the optimal (or near-optimal) purification protocols.

If ρ is of Bell-diagonal, generalized VP, or generalized Horodecki state, we have shown how to find the CSS of ρ, *say* σ, systematically by proving the following two properties: (i) The Bloch vectors of σ are identical to those of ρ. (ii) The correlation vector of σ exactly corresponds to the crossing point between the line ℓ and the geometrical object $\mathcal{L}_{r,s}$. Using these two properties, it is straightforward to find the CSS of ρ.

As we have shown in the previous section, however, these two properties are not maintained for the general two-qubit states. Therefore, in order to derive the closed formula of $E_R(\rho)$ for the arbitrary mixture ρ, we have to understand how these two properties are modified when Bloch and correlation vectors of ρ are arbitrary. The research into these issues is in progress and will be presented elsewhere.

Another interesting issue, which we will explore further, is the REE and the distillable entanglement for the higher-qubit or -qudit systems. A few years ago, the analytical expressions of the distillable entanglement were obtained for some higher-dimensional bipartite states [16–18]. Authors in those references used the upper-bound criterion $D \leqslant E_R$ and the separability property of the Smolin's unlockable state [15] in various cuts. We would like to modify Eq. (6) to be applicable not only for low-rank σ^* but also for a higher-dimensional system. If the generalization of Eq. (6) is possible, we can use it to compute the REE and the distillable entanglement for many more higher-dimensional states. It may enable us to understand the nature of the optimal (or near-optimal) purification protocols. This work is in progress too.

ACKNOWLEDGMENTS

This work was supported by a National Research Foundation of Korea grant funded by the Korean Government (2009-0073997).

[1] C. H. Bennett, G. Brassard, C. Crépeau, R. Jozsa, A. Peres, and W. K. Wootters, Phys. Rev. Lett. **70**, 1895 (1993).
[2] C. H. Bennett and S. J. Wiesner, Phys. Rev. Lett. **69**, 2881 (1992).
[3] V. Scarani, S. Lblisdir, N. Gisin, and A. Acin, Rev. Mod. Phys. **77**, 1225 (2005), and references therein.
[4] A. K. Ekert, Phys. Rev. Lett. **67**, 661 (1991).
[5] G. Vidal, Phys. Rev. Lett. **91**, 147902 (2003).
[6] M. A. Nielsen and I. L. Chuang, *Quantum Computation and Quantum Information* (Cambridge University Press, Cambridge, UK, 2000).
[7] Y. Shimoni, D. Shapira, and O. Biham, Phys. Rev. A **69**, 062303 (2004).
[8] B. P. Lanyon, M. Barbieri, M. P. Almeida, and A. G. White, Phys. Rev. Lett. **101**, 200501 (2008).
[9] E. Biham, G. Brassard, D. Kenigsberg, and T. Mor, Theor. Comput. Sci. **320**, 15 (2004).
[10] C. H. Bennett, D. P. DiVincenzo, J. A. Smolin, and W. K. Wootters, Phys. Rev. A **54**, 3824 (1996).
[11] V. Vedral, M. B. Plenio, M. A. Rippin, and P. L. Knight, Phys. Rev. Lett. **78**, 2275 (1997).
[12] V. Vedral and M. B. Plenio, Phys. Rev. A **57**, 1619 (1998).
[13] E. M. Rains, Phys. Rev. A **60**, 173 (1999).
[14] E. M. Rains, Phys. Rev. A **60**, 179 (1999).
[15] J. A. Smolin, Phys. Rev. A **63**, 032306 (2001).
[16] S. Ghosh, G. Kar, A. Roy, A. Sen(De), and U. Sen, Phys. Rev. Lett. **87**, 277902 (2001).
[17] Y. X. Chen, J. S. Jin, and D. Yang, Phys. Rev. A **67**, 014302 (2003).
[18] D. Yang and Y. X. Chen, Phys. Rev. A **69**, 024302 (2004).
[19] R. Horodecki, P. Horodecki, M. Horodecki, and K. Horodecki, Rev. Mod. Phys. **81**, 865 (2009), and references therein.
[20] M. Hayashi, D. Markham, M. Murao, M. Owari, and S. Virmani, Phys. Rev. Lett. **96**, 040501 (2006).
[21] T. C. Wei, Phys. Rev. A **78**, 012327 (2008).
[22] A. Miranowicz and S. Ishizaka, Phys. Rev. A **78**, 032310 (2008).
[23] W. K. Wootters, Phys. Rev. Lett. **80**, 2245 (1998).
[24] O. Krueger and R. F. Werner, e-print arXiv:quant-ph/0504166.
[25] R. Horodecki and M. Horodecki, Phys. Rev. A **54**, 1838 (1996).
[26] E. Jung, M. R. Hwang, D. K. Park, L. Tamaryan, and S. Tamaryan, Quantum Inf. Comput. **8**, 0925 (2008).